Diffusion Studies of Amyloid beta Peptide in bicelle

Tara George

A dissertation submitted for the partial fulfilment
of BS-MS dual degree in Science

Indian Institute of Science Education and Research Mohali
December 2015

Certificate of Examination

This is to certify that the dissertation titled **Diffusion studies of Amyloid beta peptide in bicelle** submitted by **Tara George** (Reg. No. MS10076) for the partial fulfillment of BS-MS dual degree programme of the Institute, has been examined by the thesis committee duly appointed by the Institute. The committee finds the work done by the candidate satisfactory and recommends that the report be accepted.

Prof. Sudeshna Sinha | Prof. Arvind | Dr. Kavita Dorai (Supervisor)

Dated: December 7, 2015

Declaration

The work presented in this dissertation has been carried out by me under the guidance of Dr. Kavita Dorai at the Indian Institute of Science Education and Research Mohali.

This work has not been submitted in part or in full for a degree, a diploma, or a fellowship to any other university or institute. Whenever contributions of others are involved, every effort is made to indicate this clearly, with due acknowledgement of collaborative research and discussions. This thesis is a bonafide record of original work done by me and all sources listed within have been detailed in the bibliography.

Tara George
(Candidate)

Dated: December 7, 2015

In my capacity as the supervisor of the candidates project work, I certify that the above statements by the candidate are true to the best of my knowledge.

Dr. Kavita Dorai
(Supervisor)

Acknowledgment

I am greatful to my supervisor, Dr. Kavita Dorai for giving me a chance to explore the field of NMR spectroscopy and being a wonderful guide throughout my project.
I would like to acknowledge Prof. Sudeshna Sinha and Prof. Arvind for being my committee members.

I am thankful to Dr. Sanjay Singh and his group members, specially Kuldeep for providing me the help and space for sample preparation.

Special Thanks to Satnam Singh for teaching me diffusion NMR and GROMACS. I am thankful to Navdeep Gogna for suggestions and help in sample preparation and 2 dimensional NMR experiments. I would like to Thank Shruti Dogra and Jyotsana Ojha for the helpful discussions, care and chocholates. My sincere Thanks to Harpreet singh and his chair, one of the best things in the lab. I am thankful to Debmalya Das, Amandeep Singh, Rakesh Sharma, Balbir Singh and Akshay Gaikwad for being supportive lab members. Special thanks to Vikram Sharma for two main reasons. One he has asked to thank him for coffee and for being a support during the frustuations and insomania.

My sincere thanks to my friends Lilit Jacob and Krishna K Das for being supportive especially during the last four months. I am very much thankful to Vipin, Sukanya, Rajveer, Aneeshma and Ane Nishitha for the wonderful memories and support despite of the distance.
Last but not the least my parents and brother for bearing me during the ups and downs.

List of Figures

Notation

Aβ	Amyloid beta peptide
^{1}H	Proton
^{13}C	Carbon-13
δ	chemical shift
Δ	diffusion time
ps	pico seconds
μs	micro seconds
V	potential
F	force
m	mass of the molecule
g	gradient strength
COSY	Correlation Spectroscopy
TOCSY	Total correlation spectroscopy
HSQC	Heteronuclear Single Quantum Correlation
HMQC	Heteronuclear Multiple Quantum Correlation
HMBC	Heteronuclear Multiple Quantum Correlation
NOESY	Nuclear Overhauser Effect Spectroscopy
ROESY	Rotational nuclear Overhauser Effect Spectroscopy
PEG	Polyethylene glycol
DMPC	1,2-dimyristoyl-sn-glycero-3-Phosphocholine
DHPC	1,2-diheptanoyl-sn-glycero-3-phosphocholine

Abstract

We studied the diffusion of amyloid beta peptide(25-35) inside bicelle using Pulse field gradient(PFG) Nuclear Magnetic Resonance(NMR) and molecular dynamics simulations. Amyloid beta peptide(Aβ) is the main constituent of senile plaque in the Alzheimer's disease. The neurotoxic fragment Aβ(25-35) can intercalate into the lipid bilayers and affect the dynamics of bilayers. PFG NMR experiments were conducted for samples Aβ(25-35), bicelle(DMPC/DHPC) and Aβ(25-35) inside bicelle. We calculated the diffusion coefficient for Aβ(25-35), bicelle(DMPC/DHPC) and Aβ(25-35) inside bicelle. A linear diffusion pattern was observed for Aβ(25-35) as well as bicelle alone samples. But when we incorporated Aβ(25-35) into bicelle both systems were following anomalous diffusion . The NMR experiment results were validated by molecular dynamics simulations using the MD package Groningen Machine for Chemical Simulations(GROMACS). We did 2-dimensional homonuclear and heteronuclear NMR experiments for studying the structure of Aβ(25-35) in bicelle.

Contents

Chapter 1

Introduction

1.1 NMR Phenomenon

The basis of any spectroscopic technique is that the transition of electron or any nuclear spins may be associated with the emission or absorption of energy in the form of radiation. In NMR the radiation emitted will have a frequency proportional to the applied magnetic field. Nuclear Magnetic Resonance is a phenomenon occurs when a nuclei immersed in static magnetic field is exposed to a second oscillating magnetic field. It involves quantum mechanical properties of the nucleus. All nucleons possess an intrinsic property called spin(I). A non zero spin is always associated with non zero magnetic moment. Nuclei having even number of protons and neutrons will have zero magnetic moment. Thus do not exhibit nuclear magnetic resonance.[BM94] The nuclear magnetic moment is given by,

$$\mu = \gamma I \hbar \tag{1.1}$$

where γ is the gyromagnetic ratio which determines the resonant frequency of a nucleus when an external magnetic field is applied. When a spin $\frac{1}{2}$ nucleus interacts with the magnetic field it give rise to two energy levels α and β which is characterized by azimuthal quantum number m = $\frac{1}{2}$ (spin up) and m = -$\frac{1}{2}$ (spin down). The interaction energy of a magnetic moment in a magnetic field B_0 is

$$E = -\mu.B_0 \tag{1.2}$$

Therefore

$$E = -\gamma I \hbar B_0 \tag{1.3}$$

For spin up level, energy $E_\alpha = -\frac{\hbar}{2}\gamma B_0$ and for spin down level, $E_\beta = \frac{\hbar}{2}\gamma B_0$ The energy difference between two levels, α and β

$$\Delta E = \gamma \hbar B_0 \tag{1.4}$$

From Plancks law

$$\Delta E = h\nu \tag{1.5}$$

which implies

$$\nu = \frac{\gamma B_0}{2\Pi}$$

or

$$\omega = \gamma B_0$$

where ω is the Larmor frequency of the molecule. Therefore energy associated with a spin flip can be written as

$$\Delta E = \hbar\omega \tag{1.6}$$

Larmor frequency is the frequency at which angular momentum vector of the nuclei precesses about the axis of the applied magnetic field.
The energy levels α and β are unequally populated. The ratio of the population is given by Boltzmann equation:

$$\frac{N_\beta}{N_\alpha} = e^{-\frac{\Delta E}{k_B T}} \tag{1.7}$$

N_α and N_β are population of energy levels α and β. K_B is the Boltzmann constant.

1.2 Vector Model

When a nuclei with a non zero magnetic moment enters an external magnetic field it either align itself with the field or oppose the field. Since it requires more energy to oppose the field most of the nuclei will align with the field rather than oppose it. It results in a bulk magnetic moment which is the sum of all individual magnetic moments along the direction of the applied field. This bulk magnetization can be represented by a vector pointing along the direction of the magnetic field (Z).[Kee02]

1.2.1 Larmor Precession

When an RF pulse is applied to the sample, the magnetization vector get tilted away from the Z axis(direction of applied magnetic field) by an angle β. The magnetic

vector will start rotating about the Z-axis describing a cone. The magnetic vector is said to precesses about the magnetic field known as Larmor precession. Frequency of this particular motion is termed as larmor frequency.
If the applied magnetic field is B_0 then the larmor frequency ω_0 (in rad/s) is given by,

$$\omega_0 = \gamma B_0 \tag{1.8}$$

Or in Hz

$$\nu_0 = \text{-}\frac{1}{2\pi}\gamma B_0$$

Larmor precession in rotating frame

In the fixed frame the precession frequency is at ω_0 . If we choose the rotating frame frequency to be the same then the magnetization vector will appear not to move in the rotating frame. The difference in the rotating frame frequency(ω_{rot}) and larmor frequency in the fixed frame is known as offset(Ω).

$$\Omega = \omega_0 - \omega_r ot \tag{1.9}$$

In terms of apparent magnetic field(ΔB), which is different from applied magnetic field in rotating frame,

$$\Omega = \gamma \Delta B$$

1.3 Relaxation

The tendency of an excited magnetization to return to its equilibrium position is known as relaxation. In other words it describes how quickly spins will forget the direction of orientation. Bloch theorem assumes that the equilibrium will be approached exponentially. The magnetization will decay according to:

$$\frac{dM_Z}{dt} = \frac{M_0 - M_Z}{T_1} \tag{1.10}$$

$$\frac{dM_x}{dt} = -\frac{M_x}{T_2} \tag{1.11}$$

$$\frac{dM_y}{dt} = -\frac{M_y}{T_2} \tag{1.12}$$

where M_0 is the magnetization at thermal equilibrium.
And M_x, M_y and M_z are magnetizations along the x,y and z axes respectively. T_1 and T_2 are relaxation times.[Eva95]

1.3.1 Longitudinal Relaxation T_1

The recovery of the magnetization along the Z axis is known as the longitudinal relaxation. Thus M_z is given by,

$$M_z = M_0(1 - e^{-\frac{t}{T_1}}) \tag{1.13}$$

The magnetization reappears along Z-axis after a time constant T_1 .

1.3.2 Transverse Relaxation T_2

If we have created some transverse magnetization by applying a 90° pulse, it will decay to zero overtime. Therefore the free induction signal resulting from the precession of magnetic vector in the XY plane will decay in amplitude. The loss of XY magnetization is known as transverse relaxation. In general T_2 is always greater than T_1. The transverse magnetization will decay as,

$$M_{xy}(t) = M_{xy}(0)e^{-\frac{t}{T_2}} \tag{1.14}$$

1.4 Chemical Shift(δ)

The frequency of the absorption line is linearly dependent on the strength of magnetic field.Therefore it will appear in different positions according to the spectrometer frequency. To account for this we will quote the resonance frequency of a compound with respect to a standard compound termed as chemical shift of a nuclei. Nuclei with different chemical environments resonates at different frequency. The chemical shift hamiltonian for a single spin is

$$H = \omega I_{1z} \tag{1.15}$$

The chemical shift(δ) in ppm is given by

$$\delta = \frac{\omega - \omega_{ref}}{\omega_{ref}} * 10^6 \tag{1.16}$$

ω is the larmor frequency of the nuclei and ω_{ref} is the larmor frequency of reference compound.

1.5 J Coupling

J coupling provides direct spectral manifestation of chemical bond. A measurable J coupling between two nuclei indicates a direct chemical bond. The J coupling hamiltonian between spin 1 and spin 2 is given by

$$H_{12} = 2\pi I_1.J_{12}.I_2 \tag{1.17}$$

J_{12} is the J coupling tensor. [uR08]In an isotropic liquid this is averaged by the molecular tumbling. Isotropic J coupling or scalar coupling term can be written as

$$J_{12} = \frac{1}{3}(J^{12}_{xx} + J^{12}_{yy} + J^{12}_{zz}) \tag{1.18}$$

Scalar indicates that the term is independent of molecular orientation. Unlike chemical shift the J coupling is independent of magnetic field. If the sign of J coupling term is positive it makes a positive contribution to the energy when the spins are aligned parallel and a negative contribution when they are antiparallel. A negative term implies negative contribution to the energy when the spin polarizations are parallel and a positive contribution when polarizations are antiparallel.

1.6 Dipolar coupling

Dipolar coupling results from each spin generating magnetic field that is oriented parallel to the nuclear spin vector. Two spins close in space can experience each others magnetic field which will cause variation in the effective magnetic field depend on the orientation of the dipole. Dipole-dipole interaction can be either intermolecular or intramolecular. The hamiltonian for a system of two spins which are coupled through space,

$$H_{12} = b_{12}(3(I_1.e_{12})(I_2.e_{12}) - I_1.I_2) \tag{1.19}$$

The dipole-dipole coupling constant b_{12} is given by

$$b_{12} = -\frac{\mu_0}{4\pi}\frac{\gamma_1\gamma_2\hbar}{r^3_{12}} \tag{1.20}$$

where r_{12} is the distance between two spins, γ_1 and γ_2 are gyromagnetic ratio of the spins. Structure and conformation of a molecule can be determined by measuring the through space coupling of many spin pairs. Since all other parameters are known internuclear distances can be calculated from this term.
In an isotropic liquid the short range intermolecular dipole-dipole coupling average out to zero because of the translation of the molecule. But the long range dipole-dipole coupling constant do not average out. But these coupling constants are very small.[Lev07]

1.7 Amyloid Beta peptide

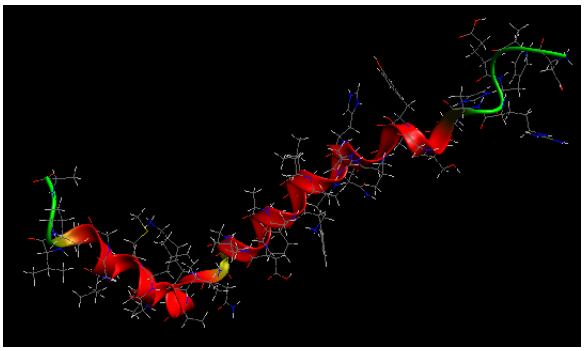

Figure 1.1: Ref:1IYT.pdb, solution structure of Aβ(1-42)

The peptide Amyloid beta is the main component of the plaques found in the brains of Alzheimer's disease patients. They can form flexible water soluble oligomers.[KSU12] The full length peptide Aβ(1-42) deeply intercalates into the the membrane, destabilizes the membrane and induces membrane fusion.
The structure of Aβ has been extensively studied in solution. Aβ generally forms α helical structure in organic solvents. In aqueous buffer or water it is predominantly β sheet. Aβ(1-40) in membrane mimicking solvents have revealed the existence of helices between residues 15 and 36 or 35 with a kink at residues 25-27 or loop at 24-30. Another study has shown that Aβ 1-40 and 1-42 containing helices[SV01] at 10-24 and 28-42. The difference in these results can be attributed to differences in pH and solvent.
β sheet structure is linked to insolubility and related to neurotoxicity. It is thought that the Aβ peptide undergoes a conformation switch from α helical to β sheet strucure during Amyloidogenesis. Assembly of amyloid fibrils appears to be a complicated

process which is still poorly understood. The mechanism of assembly of Amyloid fibrils and exact morphology remains unclear. Understanding the conformational properties and the mechanisms triggering aggregation of the Aβ peptide is of crucial importance for designing crucial theraputic agents.[Ser00]
Amyloid fibrils are physically stable self-assemblies. Investigating the structure and dynamics of Amyloid fibrils at atomic level is a challenging task because of the high molecular weight and heterogeneous properties.[YYG10]
Biology of Aβ is linked with its interaction with membrane. Studies were conducted for studying the effect Aβ on lipid membrane and effect of ions during these interactions.[TLLS06] It was found that incorporated peptides disrupted the membrane structure rather than associated peptides. It is suspected that the unusual lipid-peptide interaction mediated in the presence of ions can lead to aggregation.

1.7.1 Amyloid beta peptide(25-35)

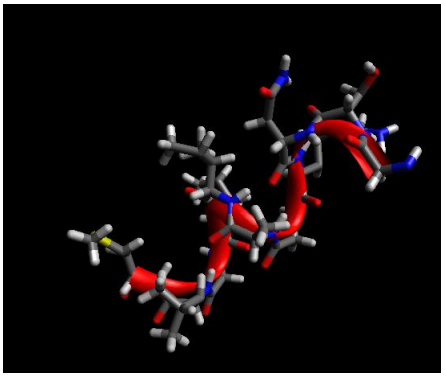

Figure 1.2: Ref:1QYT.pdb, α helical Aβ(25-35)

The fragment, Aβ(25-35) is thought to be the main responsible region for the neurotoxic effect of Aβ(1-42).Aβ(25-35) has the sequence Gly25-Ser26-Asn27-Lys28-Gly29-Ala30-Ile31-Ile32 -Gly33-Leu34-Met35. Studies have shown that this fragment shows a β sheet structure in TFE and aqueous solution.
It is shown that Aβ(25-35) increases the lateral diffusion coefficient of lipids. It can also increase the short range flexibility of the lipid membrane.[ABD10]
It was shown that monomeric form of Aβ(31-35) and Aβ(25-35) are neurotoxic and posses the ability to enter within the cells. It can determine mitochondrial damage with an evident signal for apoptosis. This can be dependent on the redox behaviour of Met35[MEC05]

1.8 Bicelle

Lipid bilayer is a thin polar membrane made of two layers of lipid molecules. These membranes form a continuous barrier around cells. The lipid bilayer is the barrier that keeps ions, proteins and other molecules where they are needed and prevents them from diffusing it into areas where should not to be. Width of the bilayer is a few nanometers.

Chapter 2

2-Dimensional NMR experiments

The conventional nmr or 1D NMR is a plot between intensity Vs frequency. In 2-dimensional NMR intensity is plotted as a function of two frequencies say F_1 and F_2. 2D NMR spectra provide more information about a molecule compared to 1D NMR and are useful in determining the structure of a molecule. In one-dimensional NMR couplings give rise to multiplets as in 2-D NMR cross peaks implies couplings. General scheme for 2D NMR

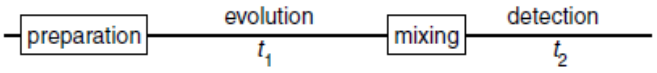

Figure 2.1: general scheme for 2D NMR experiments. Source: Keeler

During the preparation time sample is excited by one or more pulses. The resulting magnetization is allowed to evolve for time t_1 (evolution time). Following the evolution time there is a period of mixing which consists of a pulse or a set of pulses. The signal is recorded after mixing time during the detection time. The nature of the spectrum is determined by the pulses applied during preparation and mixing time. In fig.2.2a the

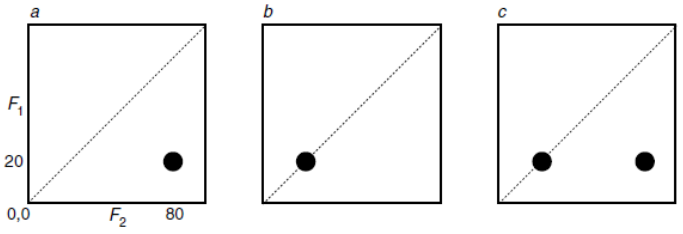

Figure 2.2: source: Keeler.

signal present during t_1 which evolved with a frequency of 20Hz. During the mixing

time this same signal was transferred in some way to another signal which evolved at 80Hz during t_2. The signal in fig.2.2b evolved with a frequency of 20Hz during t_1 as well as t_2. According to spectrum c (fig.2.2c) the signal present during t_1 evolved at 20Hz and during the mixing period, part of it was transferred into another signal which evolved at 80Hz during t_2. [Kee02]The other part remained unaffected and continued to evolve at 20Hz. Cross peak represents the part that changes the frequency during mixing time. Diagonal peak is the part that doesnt change the frequency. If there was no mixing time then the spectrum will consists only of diagonal peaks.

2.1 Homonuclear through bond correlation methods

In Homonuclear through bond correlation or scalar couplings we observe magnetization transfer between the nuclei of the same type which are connected through bonds.

2.1.1 Correlation Spectroscopy (COSY)

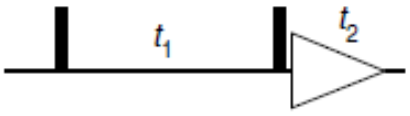

Figure 2.3: Pulse sequence for COSY. Rectangles represent 90° pulses.(source: Keeler)

COSY spectra consists of two types of peaks, diagonal peaks and cross peaks. Diagonal peaks correspond to 1 dimensional NMR. Cross peaks result from the scalar coupling of the nuclei. Cross peaks are symmetrical about the diagonal in COSY.

Consider a weakly coupled two spin system. A 90° pulse along the X axis generate a magnetization along the Y direction (assuming initial magnetization along Z axis.)

$$I_{1Z} + I_{2z} \xrightarrow{\frac{\pi}{2}} -I_{1y} - I_{2y}$$

During time t_1 spin 1 and 2 evolve as given below,

$$-I_{1y} - I_{2y} \xrightarrow{\Omega_1 t_1 I_{1z} + \Omega_2 t_1 I_{2z} + 2\pi J_{12} t_1 I_{1z} I_{2z}}$$

$[-I_{1y}cos(\Omega_1 t_1) + I_{1x}sin(\Omega_1 t_1) - I_{2y}cos(\Omega_2 t_2) + I_{2x}sin(\Omega_2 t_1)]cos\pi J_{12} t_1 +$
$[2I_{1x}I_{2z}cos(\Omega_1 t_1) + 2I_{1y}I_{2z}sin(\Omega_1 t_1) + 2I_{1z}I_{2x}cos(\Omega_2 t_1) + 2I_{1z}I_{2y}sin(\Omega_2 t_2)]sin\pi J_{12} t_1$

Following a second 90° pulse along the X axis and the previous state becomes,

$[I_{1x}sin(\Omega_1 t_1) + I_{2x}sin(\Omega_2 t_1)]cos\pi J_{12} t_1 - [2I_{1y}I_{2z}sin(_1 t_1) + 2I_{1z}I_{2y}sin(\Omega_2 t_1)]sin\pi J_{12} t_1$

In summary the two dimensional COSY map will have appearance as shown in fig.2.4.

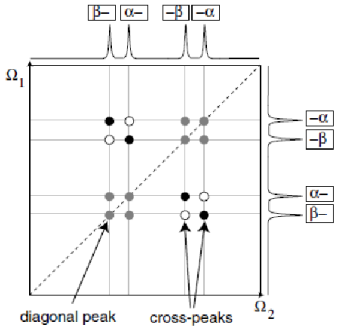

Figure 2.4: COSY of an AX system. (source: Keeler).

Thus cross peaks are dispersed by two different chemical shifts in both dimensions reducing the chance of overlapping of resonances. [Kee02]

2.1.2 Total Correlation Spectroscopy (TOCSY)

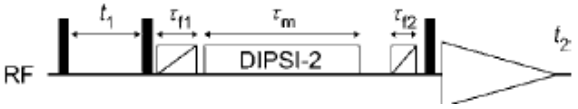

Figure 2.5: Pulse sequence for TOCSY. (source: Keeler)

Total correlation spectroscopy relies on cross polarization rather than the coherence transfer methods. In conventional COSY experiment coherence transfer is only possible between protons on the adjacent atoms where as in TOCSY the protons are able to relay the coherence so that it is transferred among all the protons that are connected by adjacent atoms. TOCSY is used in large molecules with many separated

coupling networks such as peptides, proteins, oligosaccharides, polysaccharides.[JC95]

The TOCSY pulse sequence (fig.2.5) involves a modified spin lock (DIPSI in fig.2.5). The spin locking field causes cross-polarization or an oscillatory exchange of magnetizations between the two spins which experience identical local RF fields. Thus the spins become temporarily equivalent. There are two types of spin lock sequences, isotropic mixing and Hartmann-Hahn-mixing (HOHAHA). Istropic mixing leads to spectra with mixed phases where as the latter lead to a pure phase spectrum. For a simple two spin system, complete exchange of magnetization occurs for a contact time of 1/2J where J is the scalar coupling constant between two spins. The HOHAHA variants simply involves alternative decoupling schemes during spin lock period. The schemes which are commonly employed are include composite pulses such as MLEV-17 and DIPSI-X.[Kee02]

2.2 Heteronuclear through bond correlation experiments

This method gives information on the correlation of two different types of nuclei, (say^1H and ^{13}C). The resultant two dimensional spectra will consist of peaks whose coordinates are given by chemical shift of one type of nucleus in one dimension(^1H) and chemical shift of another nucleus which is coupled to the first nucleus, in the second dimension(^{13}C).

2.2.1 Heteronuclear Multiple Quantum Correlation (HMQC)

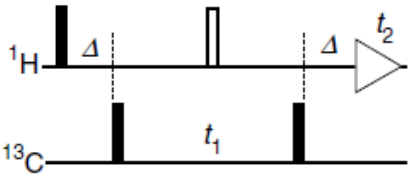

Figure 2.6: HMQC pulse sequence. Open rectangle for 180 pulse.(source: Keeler)

The pulse sequence for HMQC is given in fig.7. For the purpose of analysis we take ^1H as spin 1 and ^{13}C as spin 2. (ref.1)

We start the analysis with spin 1. Assuming the equilibrium magnetization of spin 1 is along z axis after 90° pulse the becomes $-I_{1y}$. Since the pulse sequence applied to the spin 1 is similar to a spin echo sequence (90-τ-180-τ) the state of the system at the end of the delay Δ is simply due to evolution of $-I_{1y}$ under scalar coupling,

$$-I_{1y}cos(\pi J_{12}\Delta) + 2I_{1x}I_{2z}sin(\pi J_{12}\Delta)$$

where $\Delta = 1/2J_{12}$. Therefore only the second term remains.

The second 90° pulse applied to spin 2 leads to,

$$2I_{1x}I_{2z} \xrightarrow{\frac{\pi}{2}I_{2x}} -2I_{1x}I_{2y}$$

This generates a mixture of heteronuclear double and Zero quantum coherence which then evolves at t_1. It is already noted that spin 1 will be refocused after the 180° pulse. So the evolution under spin 1 offset can be ignored. Addition to that spins i and j in multiple quantum coherence does not evolve under the influence of the coupling between these two spins, J_{12}. Therefore only evolution of spin 2 under the offset should be taken into account.[Eva95]

$$-2I_{1x}I_{2y} \xrightarrow{\Omega_1 t_1 I_{2z}} -2I_{1x}I_{2y}cos(\Omega_2 t_1) + 2I_{1x}I_{2x}sin(\Omega_2 t_1)$$

A second 90° pulse to spin 2, no effect on the second term and first term will transform as,

$$-2I_{1x}I_{2y}cos(\Omega_2 t_1) \xrightarrow{\frac{\pi}{2}I_{2x}} -2I_{1x}I_{2z}cos(\Omega_2 t_1)$$

This term evolves under coupling.

$$-2I_{1x}I_{2z}cos(\Omega_2 t_1) \xrightarrow{2\pi J_{12}\Delta I_{1z}I_{2z}} -I_{1y}cos(\Omega_2 t_1)$$

In F_2 there will be a doublet centered at the offset of spin 1 and these peaks will have an F_1 coordinate simply determined by the offset of spin 2.

2.2.2 SOFAST HMQC

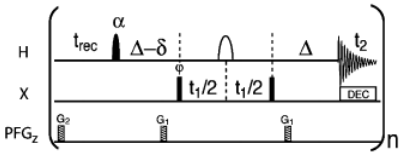

Figure 2.7: Pulse sequence for SOFAST-HMQC. (source: Schada et.al)

This sophisticated experiment can acquire data in a very few seconds with high resolution. Mostly used for studying protein folding and observation of short lived protein intermediates.[SB05]

2.2.3 Homonuclear multiple bond correlation (HMBC)

In HMBC experiments the correlation between proton and carbon those are connected by two or three bonds are studied. It can show correlations between amide hydrogen to α proton.

2.3 Homonuclear through space correlation methods

In these experiments coherence transfer occurs through space (dipolar coupling). They exhibit cross peaks for all protons that are close in space.

2.3.1 Nuclear Overhauser Effect Spectroscopy (NOESY)

Figure 2.8: Pulse sequence for NOESY.$\tau_m ix$ is the mixing time. (source: Keeler)

NOESY spectra is similar to COSY with cross peaks and diagonal peaks with cross relaxation through space. Nuclear Overhauser Effect is the transfer of cross polarization from one spin to another via cross relaxation.[Eva95]

2.3.2 Rotating frame Overhauser Effect Spectroscopy (ROESY)

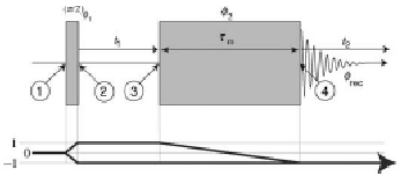

Figure 2.9: ROESY pulse sequence. (source: Levitt)

The pulse sequence of ROESY is similar to TOCSY. However the RF power to achieve spin locking is much lower compared to TOCSY. This helps to prevent the appearance of TOCSY cross peaks in the resulting spectrum. In ROESY experiments the intensity increases with correlation time. This is due to the fact that cross relaxation occurs in the presence of a weak rf field rather than a large static magnetic field. [Lev07]

2.4 Results

Homonuclear and heteronuclear 2 dimensional NMR experiments were done for 2mM of Aβ(25-35) in 80mM DMPC and 160mM DHPC.

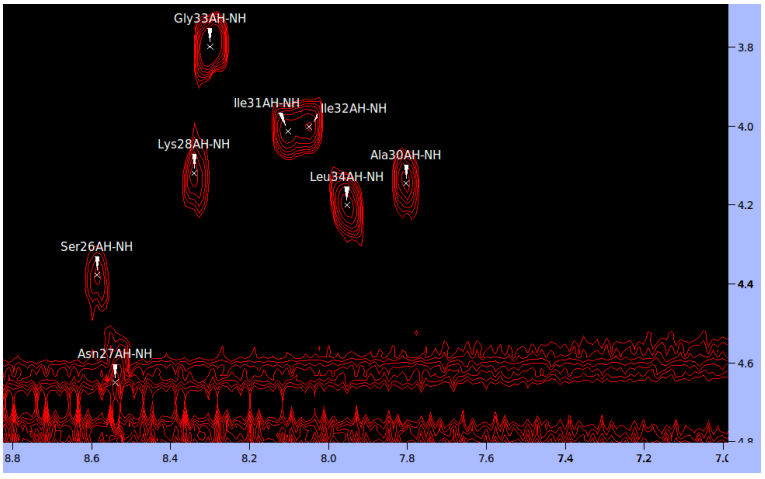

Figure 2.10: COSY spectra for the Aβ(25-35) in bicelle. assignments matching with [V.B08]

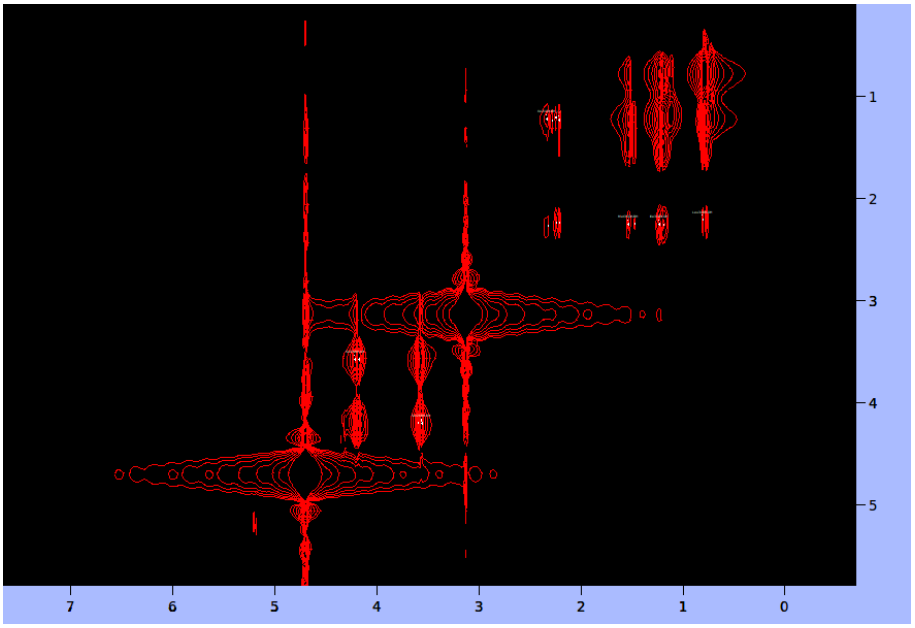

Figure 2.11: TOCSY spectra for the Aβ(25-35) in bicelle

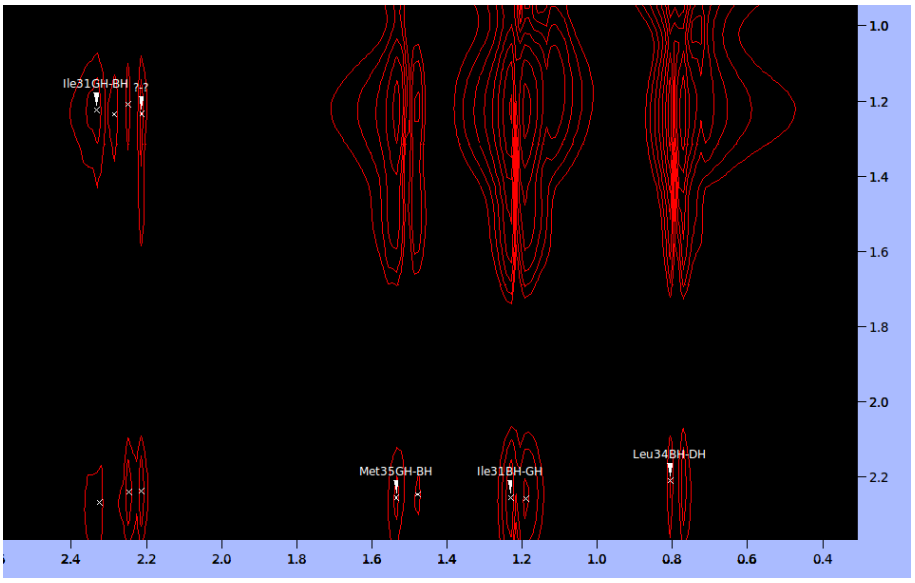

Figure 2.12: TOCSY spectra for the Aβ(25-35) in bicelle peaks labeled. (region 1)

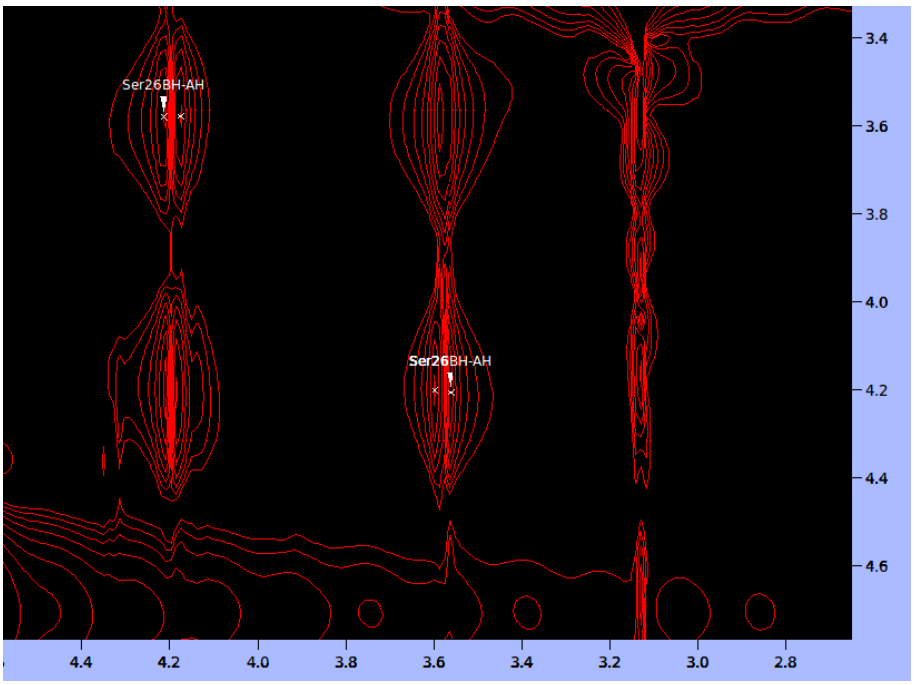

Figure 2.13: TOCSY spectra for the Aβ(25-35) in bicelle peaks labeled. (region 2)

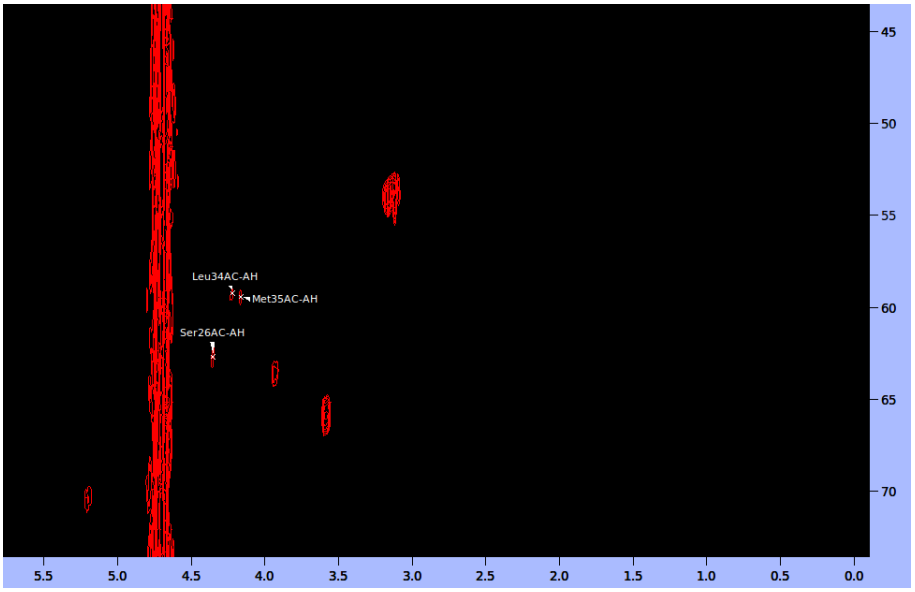

Figure 2.14: HMQC spectra for the Aβ(25-35) in bicelle

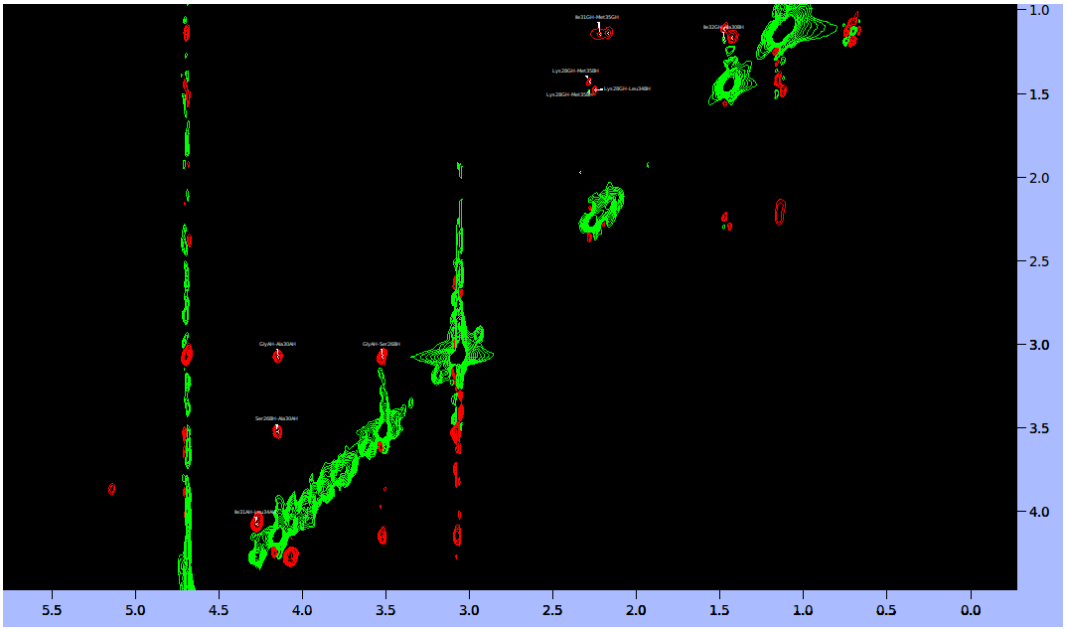

Figure 2.15: ROESY spectra for the Aβ(25-35) in bicelle

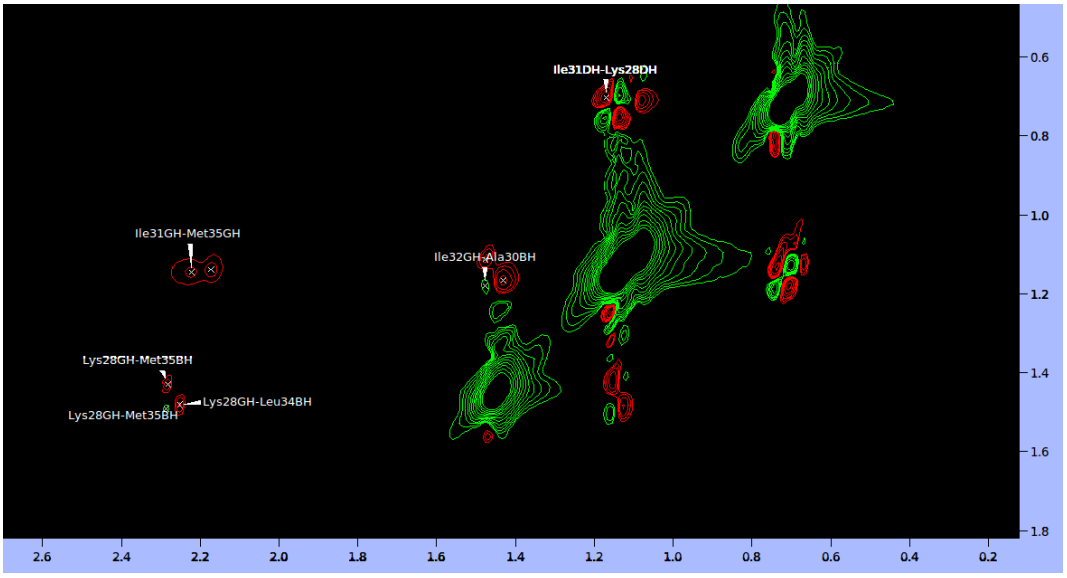

Figure 2.16: ROESY spectra for the Aβ(25-35) in bicelle peaks labeled. (region 1)

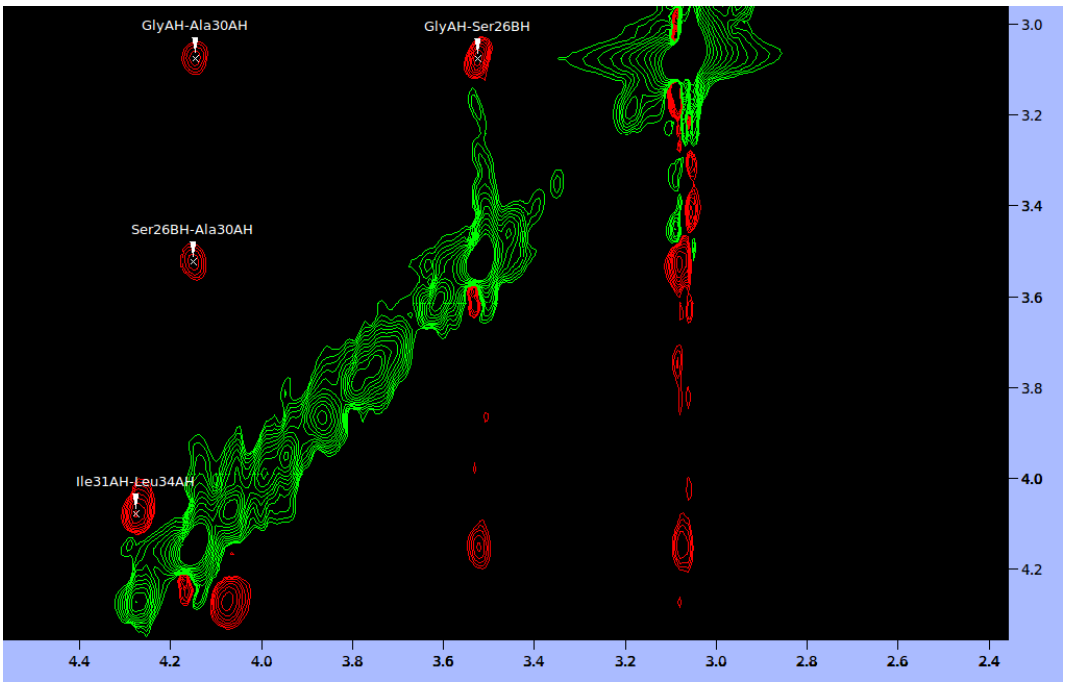

Figure 2.17: ROESY spectra for the Aβ(25-35) in bicelle peaks labeled. (region 2)

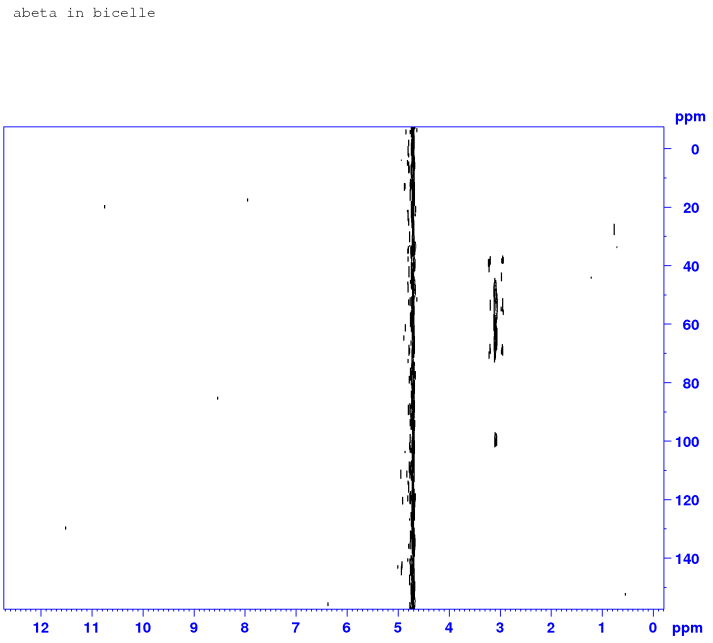

Figure 2.18: HMBC spectra for the Aβ(25-35) in bicelle

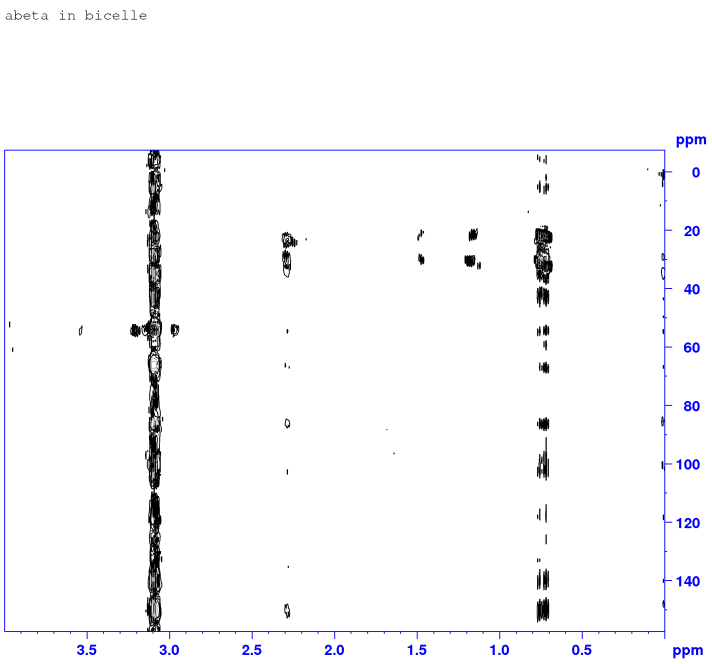

Figure 2.19: HMBC spectra with water suppression for the Aβ(25-35) in bicelle

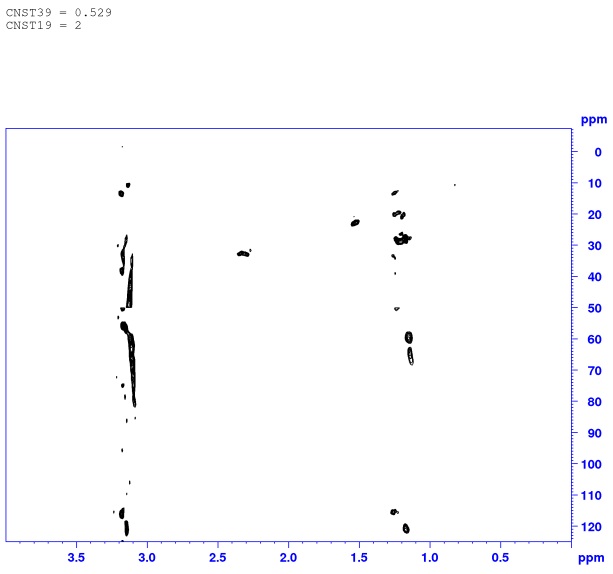

Figure 2.20: SOFAST-HMQC spectra for the Aβ(25-35) in bicelle

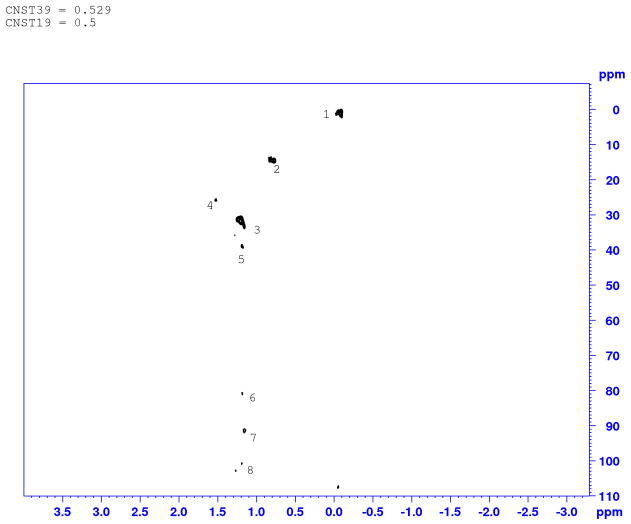

Figure 2.21: SOFAST-HMQC spectra for the Aβ(25-35) in bicelle

2.5 Conclusion

The amino acid sequence of the peptide , Gly25-Ser26-Asn27-Lys28-Gly29-Ala30-Ile31-Ile32-Gly33-Leu34-Met35. The COSY spectrum showed through bond correlations of protons in the constituent amino acids of A(25-35). In TOCSY correlation between protons of Ser26 as well as Lys28 were observed. HMQC exhibited 13C to 1H coupling of Ser26, Ile32 and Lys28. ROESY was done to figure out the protons which are correlated through space(dipolar coupling).[BM94] We inferred from the ROESY spectrum that Ile31-Lys28, Ile32-Ala30, Ile31-Met35, Lys28-Met35, Lys28-Leu34 and Ser26-Ala30 are spatially close.

Chapter 3

Diffusion NMR of Aβ (25-35) in bicelle

Diffusion is the random translational motion of molecules or ions that is driven by internal thermal energy. It is the basic mechanism by which molecules are distributed in space. A distinguishing feature of diffusion is that it results in mixing or mass transport of molecules without a bulk motion.

3.1 Normal diffusion

Normal diffusion or free diffusion is the random movement of particles. It is mostly dependent on the gradient of the macroscopic properties.

3.1.1 Brownian model of diffusion

The theory of Brownian motion is one of the simplest approach to study the diffusion of a system. The random motion of a small particle immersed in a fluid is called Brownian motion.[Zwa01]
Diffusion can be considered as random walk of molecules. In a one dimensional random walk there are 2^n possible trajectories. Number of trajectories that give R steps towards right side:

$$nC_R = \frac{n!}{R!(n-R)!} \tag{3.1}$$

Probability of finding a particle at k after n steps:

$$W(k,n) = \frac{n!}{2^n(\frac{n+k}{2})!(\frac{n+k}{2})!} \tag{3.2}$$

which can also be expressed as

$$W(k,n) = \frac{1}{\sqrt{2\pi n}} e^{-\frac{k^2}{n}} \tag{3.3}$$

Mean displacement of a particle after n random steps, $\langle X_n \rangle = 0$
Mean square displacement of a particle executing 1 dimensional random walk is linear with time.

$$\langle X_n^2 \rangle = 2Dt \tag{3.4}$$

This relation is also known as 1 dimensional diffusion law. It can also be written as

$$\langle X_n^2 \rangle = \langle (X_{n-1} + k_n L)^2 \rangle = \langle (X_{n-1})^2 \rangle + 2L\langle X_{n-1} k_n \rangle + L^2 \langle k_n^2 \rangle \tag{3.5}$$

where L is the length of each step, $k_n = \pm 1$ with equal probability. The above equation can be reduced to,

$$\langle X_n^2 \rangle = NL^2 \tag{3.6}$$

N is the total number of steps. Comparing eqn 3.4 and eqn 3.6 diffusion coefficient D can be written as,

$$D = \frac{L^2}{2\Delta t} \tag{3.7}$$

In 2 dimension mean square displacement of a random walk, $\langle r_n^2 \rangle = \langle x_n^2 \rangle + \langle y_n^2 \rangle = 4\text{Dt}$ and similarly in 3 dimension it is given by $\langle r_n^2 \rangle = 6\text{Dt}$.

3.1.2 Fick's Laws of diffusion

Ficks first law of diffusion postulates diffusive flux goes from high concentration region to low concentration region with a magnitude proportional to concentration gradient.[Nel08]

$$\mathbf{J}(\mathbf{r},t) = -D\nabla c(\mathbf{r},t) \tag{3.8}$$

J: diffusion flux [mol/m^2s]
D: diffusion coefficient [m^2/s]
C: concentration in number of particles per unit volume [mol/m^3]

Combining *Fick's first law* with the equation of continuity,

$$\frac{\partial C}{\partial t} + \nabla.\mathbf{J} = 0 \tag{3.9}$$

we obtain **Fick's second Law of diffusion**,

$$\frac{\partial C(\mathbf{r},t)}{\partial t} = D\nabla^2 C(\mathbf{r},t) \tag{3.10}$$

Fick'Laws of diffusion are based on the assumption that the number of random particles is very large. The beauty of Fick's second Law or diffusion equation is that it is deterministic.If If we know the initial profile concentration, C(**r**,0) by solving the diffusion equation we can predict the future profile C(**r**,t).

3.1.3 Stokes - Einstein Relation

Stokes - Einstein equation is given for diffusion of a spherical particle through a fluid with low Reynolds number. **Einstein relation** gives the diffusion coefficient for a particle moving in a fluid with temperature T

$$D = \frac{k_B T}{f} \tag{3.11}$$

k_B: Boltzman constant(k_B = R/N_A; R is the gas constant and N_A is the Avogadro constant, dimension JK^{-1})
f is the viscous friction coefficient.
Viscous coefficient for a spherical object is related to its size. This relation is given by **Stokes formula**,

$$f = 6\pi\eta R \tag{3.12}$$

R : hydrodynamic radius of the particle
η :viscosity of the fluid [Pa.s]
Combining *equations* 3.11 and 3.12 we obtain *Stokes - Einstein relation*

$$D = \frac{k_B T}{6\pi\eta R} \tag{3.13}$$

3.2 Anomalous diffusion

In anomalous diffusion, the mean square displacement of a particle exhibits a non linear relationship with time in contrast to the normal diffusion. In this case the probability distribution of the molecular displacements follow non-Gaussian statistics. Mean square displacement for a 3-dimensional system with diffusion time t,

$$\langle r_n^2 \rangle = 6\mathrm{D}t^{\alpha}$$

where α is the measure of the complexity of the environment.

For a typical diffusion $\alpha = 1$.

If $\alpha > 1$, the molecule undergoes superdiffusion.

If $\alpha < 1$, the process is subdiffusion.[V.B08]

3.3 Pulsed Field Gradient NMR

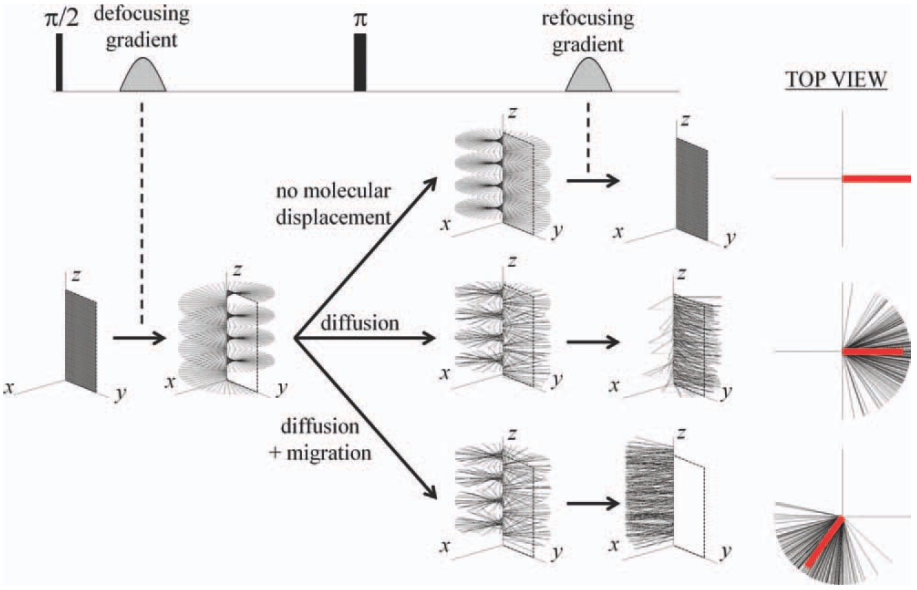

Figure 3.1: PFG Spin echo pulse sequence and its effect when there is no molecular movement, diffusion and unidirectional translation (taken from sinnavae et al)

In an ideal NMR experiment the static magnetic field(B_0) is homogeneous around the sample. But when the magnetic field is inhomogeneous the spins at different positions of the sample will precess at different frequencies around the magnetic field. Thus developing a phase difference with respect to each other which results in the

attenuation of NMR signal intensity.
Assume there a constant magnetic field gradient with strength g along the Z axis of the sample. The precessional frequency of the magnetization is then become position dependent.[Sin12]

$$\omega_g = -\gamma(B_0 + gz) = \omega_0 - \gamma gz \tag{3.14}$$

If we consider the frequency of the rotating frame to be ω_0, then only gradient induced frequency, -γgz to be taken into account. If the gradient is applied for a time δ, then the total angle swept by the magnetization while precessing is -$\gamma gz\delta$.
We assume that the transverse magnetization has the initial orientation along the Y axis.Then the evolution of the magnetization is given by,

$$M_Y \rightarrow M_Y cos(\gamma gz\delta) + M_X sin(\gamma gz\delta)$$

The X and Y components of the magnetization will depend on the position along the Z axis of the sample. The detectable magnetization remains along the Y axis while its intensity experiences a dampening in the form of a sinc function.
If we reverse the polarity of the gradient after a time delay δ (ie. The gradient strength becomes -g) then the magnetization at every position Z will get refocused after the second delay δ.

$M_Y cos(\gamma gz\delta) + M_X sin(\gamma gz\delta) \rightarrow$

$$[M_Y cos(\gamma gz\delta) - M_X sin(\gamma gz\delta)]cos(\gamma gz\delta) + [M_Y cos(\gamma gz\delta) + M_X sin(\gamma gz\delta]sin(\gamma gz\delta) = M_Y$$

Thus the loss of coherence due to gradient pulse is reversible. But if diffusion takes place during the spin echo then the molecules displace randomly along the Z axis. Now the refocusing second gradient will leave a stochastic, irreversible dephasing of magnetization along the Z axis(fig.3.1). It results in the decay of intensity of magnetization along Y axis.

3.4 Stejskal Tanner(ST) equation

The ST equation describes the signal attenuation in PFGSE experiment due to loss of coherence during diffusion as function of the experimental parameters.

- **ST equation for normal diffusion**

$$\frac{I}{I_0} = exp[-(\gamma\delta g)^2 D(\Delta - \frac{\delta}{3})] \tag{3.15}$$

where I is the Intensity of the signal
γ is the gyromagnetic ratio which is constant for a nuclei.(MHz/T)
δ is gradient pulse length(ms)
Δ is the diffuion time(ms)
g is the gradient strength(G/m^2)
D is the diffusion coefficient.[RL11]

- **ST equation for anomalous diffusion**

$$\frac{I}{I_0} = exp[-(bD)^\alpha] \tag{3.16}$$

b=$-(\gamma\delta g)^2(\Delta - \frac{\delta}{3})$
α is the index of spatial heterogeneity.[KMBH03]

3.5 Diffusion Experiments

Pulsed field gradient NMR experiment were done for the following samples on 600MHz Avance III Bruker machine.

- Sample I : 2mM of Aβ(25-35) in D_2O
- Sample II : bicelle (80mM of DMPC and 160mM of DHPC) in buffer + D_2O
- Sample III: 2mM of Aβ in bicelle in buffer + D_2O

3.6 Results

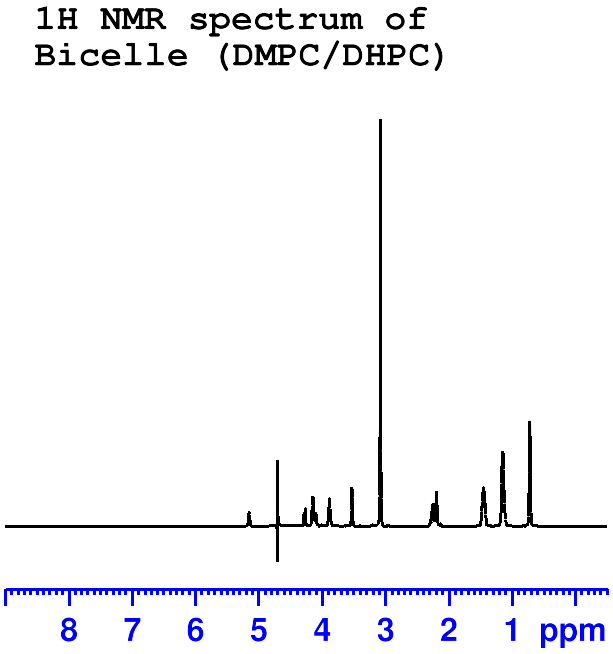
1H NMR spectrum of
Bicelle (DMPC/DHPC)
8 7 6 5 4 3 2 1 ppm

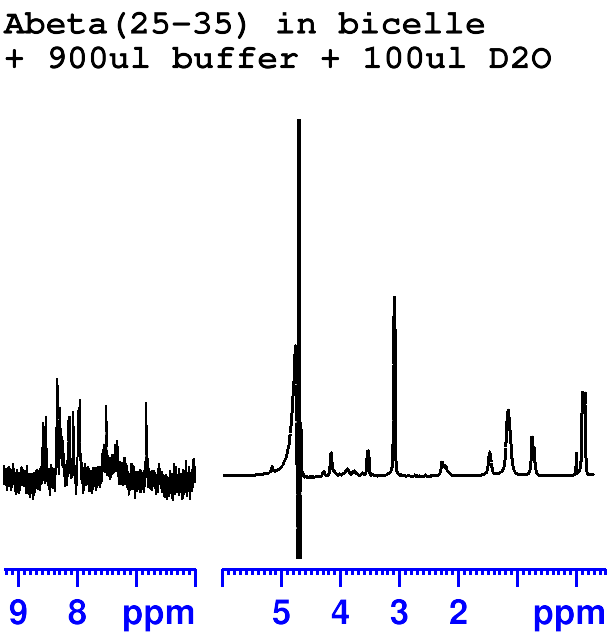
Abeta(25-35) in bicelle
+ 900ul buffer + 100ul D2O
9 8 ppm
5 4 3 2 ppm

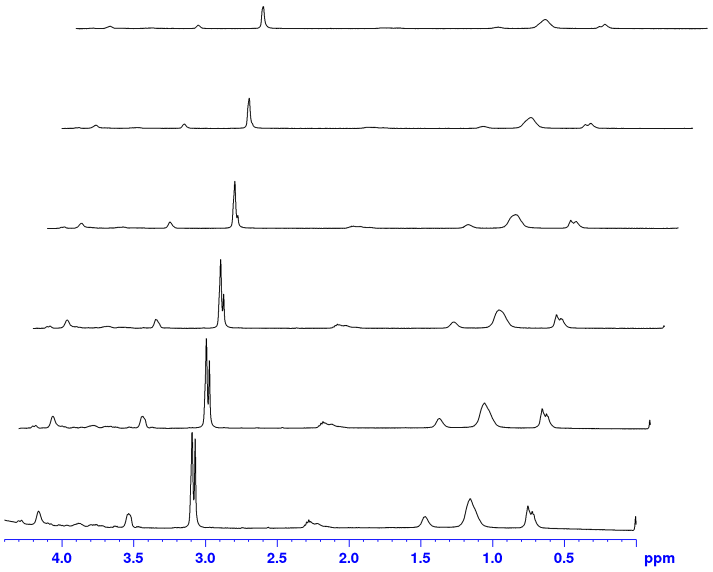

Figure 3.2: Amyloid β in bicelle spectra in decreasing order of gradient strength.

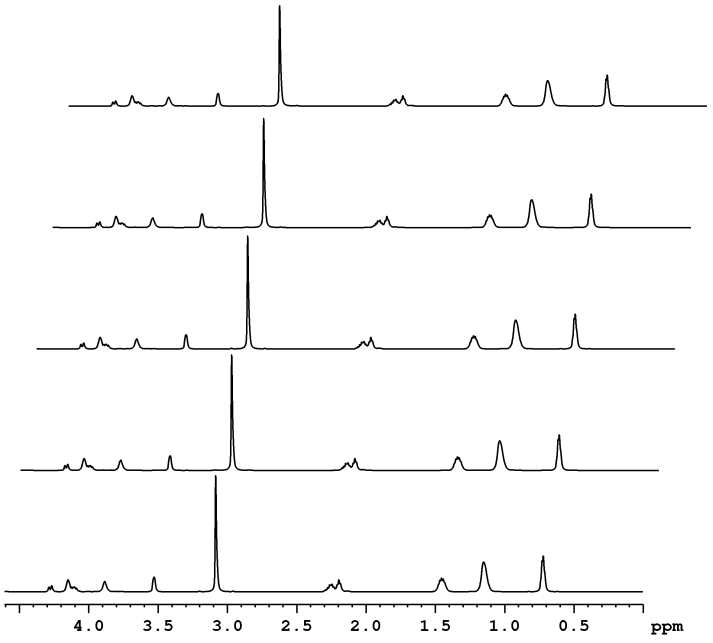

Figure 3.3: bicelle spectra in decreasing order of gradient strength.

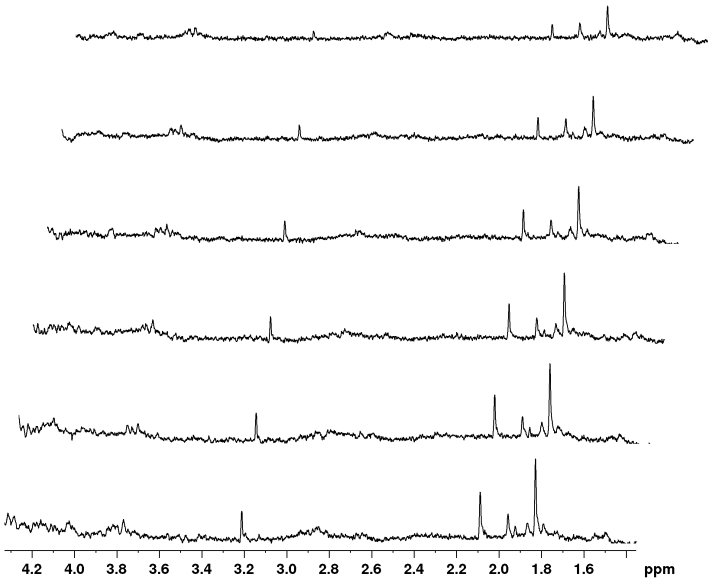

Figure 3.4: Aβ(25-35) in D_2O spectra in decreasing order of gradient strength.

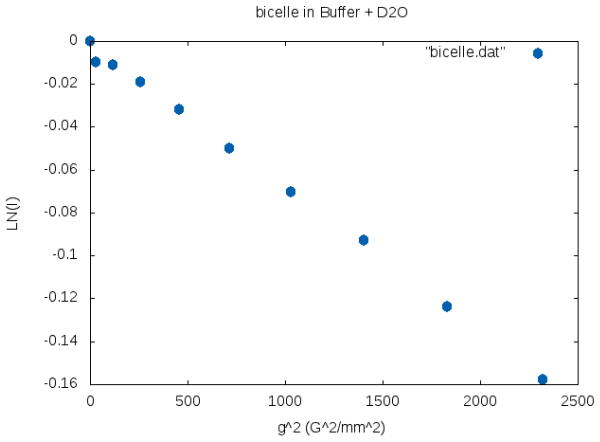

Figure 3.5: figure
g^2 V/s LN(I) plot for bicelle

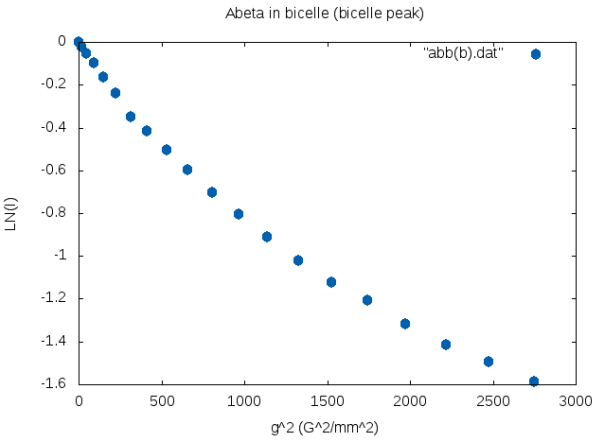

Figure 3.6: figure
g^2 V/s LN(I) plot for bicelle when Aβ is inserted

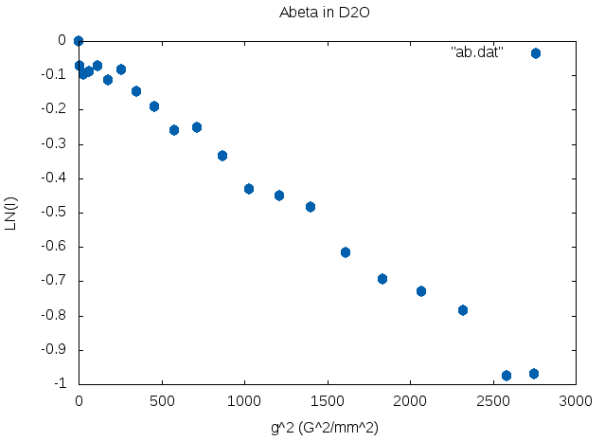

Figure 3.7: figure
g^2 V/s LN(I) plot for Aβ

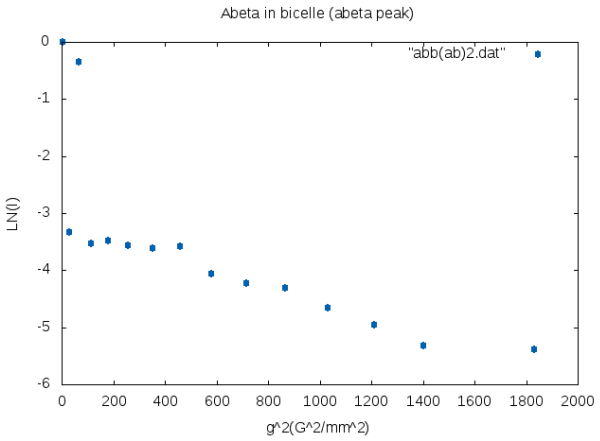

Figure 3.8: figure
g^2 V/s LN(I) plot for Aβ when inserted in bicelle

Sample	Calculated diffusion coefficient(D)	Diffusion time
Aβ in D_2O	8.8658*10^{-8} m^2/s	10ms
Aβ inside bicelle	2.7767*10^{-8} m^2/s	100ms
Bicelle only	10.3*10^{-9} m^2/s	10ms
bicelle when Aβ is inserted	8.33*10^{-9} m^2/s	100ms

3.7 Conclusion

- Self-diffusion of bicelle show a linear relation between mean square displacement and time.
- Aβ in D_2O follows linear diffusion pattern.
- Mean square displacement of Aβ in bicelle show a non linear relationship with time.

Chapter 4

Molecular dynamics simulations

Molecular dynamics is a computer simulation to study the physical movement of atoms and molecules in an N-body simulation. The atoms and molecules were interacting for a fixed period of time giving a dynamical evolution of time. MD simulations solve Newton's equations of motion for a system of N interacting particles,

$$m_i \frac{\partial^2 r_i}{\partial t^2} = F_i, i = 1, 2...N$$

The forces are negative derivatives of a potential function V($r_1, r_2, ..., r_N$)

$$F_i = -\frac{\partial V}{\partial r_i}$$

The equations are solved simultaneously in small time steps. The system is followed for some time keeping the temperature and pressure conditions, and the coordinates are written to an output file at regular intervals. After the initial changes the system will reach equilibrium. Coordinates as a function of time represents the trajectory of the system. Many macroscopic properties can be extracted from the trajectory file. Molecular dynamics simulations permit the complex dynamical process that occur in the biological systems. It includes protein stability, conformational changes, Protein folding and transport in the biological systems.[9]

4.1 MD Algorithm

Each MD or energy minimization run requires initial velocities and coordinates of all the particles involved.[9]

The global MD algorithm

- Step 1 : *Input initial conditions*
  - Interaction potential V as function of the position of atoms.
  - initial coordinates **r** of all atoms in the system
  - velocities **v** of all atoms in the system.
- Step 2 : *Compute forces*
  - Force on each atom by calculating the force between bonded interations and non bonded atom pairs. In addition effect of external forces.
  - Potential and kinetic energies and pressure tensors were calculated.
- Step 3 : Update configuration
  - Movement of atoms were simulated by numerically solving Newton's equations of motion

  2,3 and 4 repeated for *N* number of steps
- Step 4 : Output
  - final positions, velocities and energies, temperature and pressure

4.2 Potential functions

There are three types of potential functions: non-bonded, bonded and restraints.

4.2.1 Non-bonded interactions

The non-boned interactions contain a repulsion term, a dispersion term and a Coulomb term. The non-bonded interactions are computed on the basis of a neighbour list (a list of non bonded atoms with in a certain radius).
Non bonded interactions are pair-additive and centro-symmetric:

$$V(r_1, r_2, ...r_N) = \sum_{i<j} V_{ij}(r_{ij}) \tag{4.1}$$

$$F_i = -\sum_j \frac{dV_{ij}(r_{ij})}{dr_{ij}} \frac{\mathbf{r}_{ij}}{r_{ij}} \tag{4.2}$$

- **Lennard-Jones interaction**

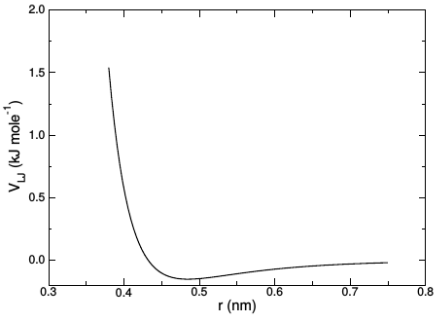

Figure 4.1: The Lennard-Jones interaction potential. Source: GROMACS manual

The Lennard-Jones potential V_{LJ} between two equal atoms

$$V_{LJ}(r_{ij}) = \frac{C_{ij}^{(12)}}{r_{ij}^{12}} - \frac{C_{ij}^{(6)}}{r_{ij}^{(6)}} \tag{4.3}$$

The parameters $C_{ij}^{(12)}$ and $C_{ij}^{(6)}$ depend on the types of atom pairs.
The force derived from this potential,

$$F_i(r_{ij}) = (12\frac{C_{ij}^{(12)}}{r_{ij}^{13}} - 6\frac{C_{ij}^{(6)}}{r_{ij}^{7}})\frac{\mathbf{r}_{ij}}{r_{ij}} \tag{4.4}$$

LJ potential can also written in the form,

$$V_{LJ}(\mathbf{r}_{ij}) = 4\epsilon_{ij}((\frac{\sigma_{ij}}{r_{ij}})^{12} - (\frac{\sigma_{ij}}{r_{ij}})^{6}) \tag{4.5}$$

where ϵ is the depth of the potential well and σ is the finite distance at which the interparticle potential is zero.

- **Buckingham Potential**

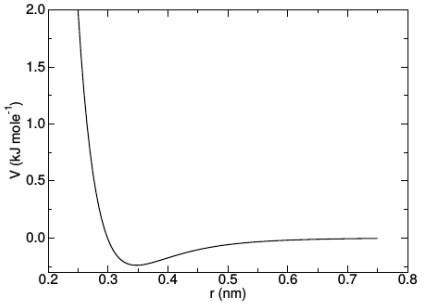

Figure 4.2: The Buckingham interaction potential. Source: GROMACS manual

Buckingham potential is given by

$$V_{bh}(r_{ij}) = A_{ij}exp(-B_{ij}r_{ij}) - \frac{C_{ij}}{r_{ij}^6} \tag{4.6}$$

and the force for this field is

$$F_i(r_{ij}) = [A_{ij}B_{ij}exp(-B_{ij}r_{ij}) - 6\frac{C_{ij}}{r_{ij}^7}]\frac{\mathbf{r}_{ij}}{r_{ij}} \tag{4.7}$$

- **Coulomb interaction**

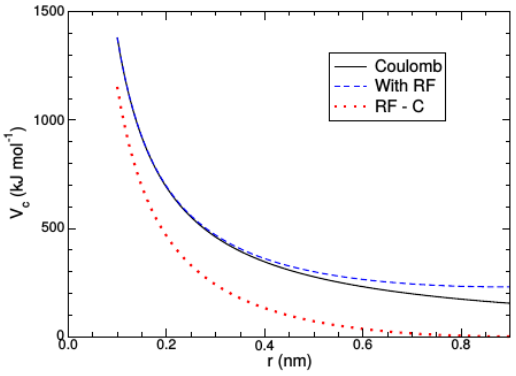

Figure 4.3: The Coulomb interaction potential with and without reaction field for charged particles with same sign. Source: GROMACS manual

For two charged particles Coulomb potential is defined as

$$V_c(r_{ij}) = \frac{1}{4\pi\epsilon_0}\frac{q_i q_j}{\epsilon_r r_{ij}} \tag{4.8}$$

The force for this interaction is given by

$$F_i(r_{ij}) = \frac{1}{4\pi\epsilon_0}\frac{q_i q_j}{\epsilon_r r_{ij}^2}\frac{\mathbf{r}_{ij}}{r_{ij}} \tag{4.9}$$

4.2.2 Bonded interactions

Bonded interaction include bond stretching, bond angle and dihedral interactions. It is mostly based on 2-body, 3-body or 4-body fixed atom lists.
The bond stretching between two covalently bonded atoms is mediated by harmonic potential. In some systems the bond stretchings are anharmonic. Those systems follow Morse potential. For the morse potential the well is asymmetric and at infinity the force is zero.

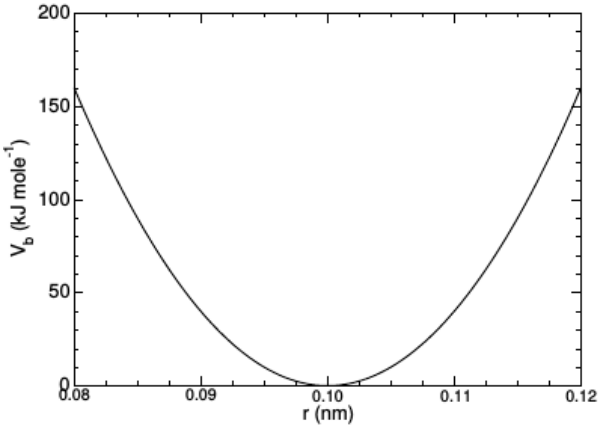

Figure 4.4: Harmonic potential for the bond stretching. source: GROMACS manual

4.3 Force field

Force field is used to generate potential energies and forces for the particles in the system. Parameters used in these equations are the second component these equations are built up on. GROMOS87, GROMOS-96, OPLS, AMBER, CHARMM and

MARTINI are some of the forcefields used in GROMACS. MARTINI forcefield is used for coarse grained simulations. it can be used for constructing systems like proteins and membranes.

4.4 Coordinates and velocities

For starting a run the coordinates, box size and velocities for all the particles in the system is required. The shape and size of the box is determined by the basis vectors. The velocities are calculated by leap frog algorithm or velocity verlet algorithm.

4.4.1 Leap frog algorithm

The positions **r** at time t and velocities **v** at time t-$\frac{1}{2}$t is used in this algorithm.[Hoc74] In leap-frog integrator the positions and velocities are updated using the following relations:

$$\mathbf{v}(t + \frac{1}{2}\Delta t) = \mathbf{v}(t - \frac{1}{2}\Delta t) + \frac{\Delta t}{m}\mathbf{F}(t) \tag{4.10}$$

$$\mathbf{r}(t + \Delta t) = \mathbf{r}(t) + \Delta t\mathbf{v}(t + \frac{1}{2}\Delta t) \tag{4.11}$$

It produces trajectories that are identical Verlet algorithms.

4.4.2 Velocity verlet algorithm

In verlet algorithm positions the equations of motions are integrated using **r** at time t and velocities **v** at time t.[Ber08]

$$\mathbf{v}(t + \frac{1}{2}\Delta t) = \mathbf{v}(t) + \frac{\Delta t}{2m}\mathbf{F}(t) \tag{4.12}$$

$$\mathbf{r}(t + \Delta t) = \mathbf{r}(t) + \Delta t\mathbf{v}(t + \frac{1}{2}\Delta t) \tag{4.13}$$

$$\mathbf{v}(t + \Delta t) = \mathbf{v}(t + \frac{1}{2}\Delta t) + \frac{\Delta t}{2m}\mathbf{F}(t + \Delta t) \tag{4.14}$$

4.5 Results

Simulations were done for Aβ(25-35) in bicelle (DMPC/DHPC) and Aβ(1-40) in bicelle using a scientific designed for molecular dynamics simulations, GROningen MAchine for Chemical Simulations (GROMACS).

4.5.1 Molecular dynamics simulations of Aβ(25-35) in bicelle

Martini coarse grained force field was used for the molecular dynamics simulations[RG]. The simulation was run for 0.3μs at 298 K. Volume of the simulation box was 216nm^3. 3 molecules of Aβ(25-35), 144 molecules of DMPC, 288 molecules of DHPC and 15000 water molecules constitute the system.

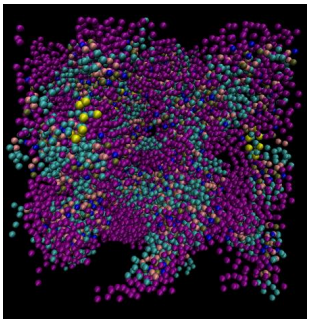

Figure 4.5: The system Aβ(25-35) in bicelle before simulation,pink:water, Aquamarine:Phospholipids, Yellow: Aβ(25-35)

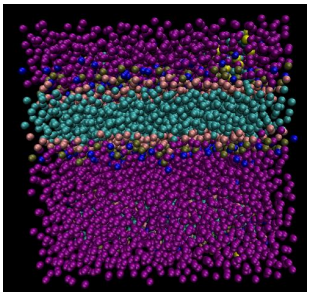

Figure 4.6: The system Aβ(25-35) in bicelle after simulation,pink:water, Aquamarine:Phospholipids, Yellow: Aβ(25-35)

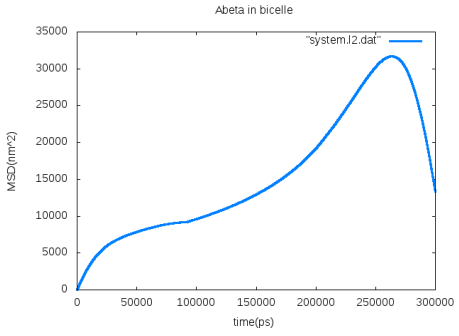

Figure 4.7: Mean square displacement V/s time for the system Aβ(25-35) in bicelle

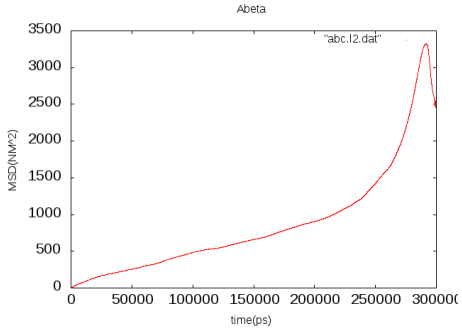

Figure 4.8: Mean square displacement V/s time for Aβ(25-35) in the system Aβ(25-35) in bicelle

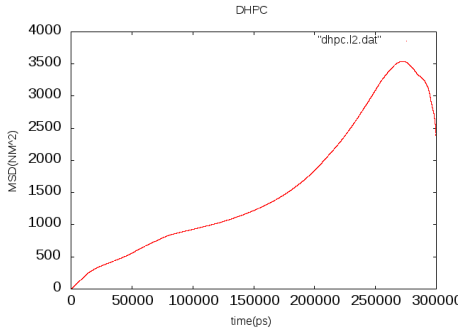

Figure 4.9: Mean square displacement V/s time for DHPC in the system Aβ(25-35) in bicelle

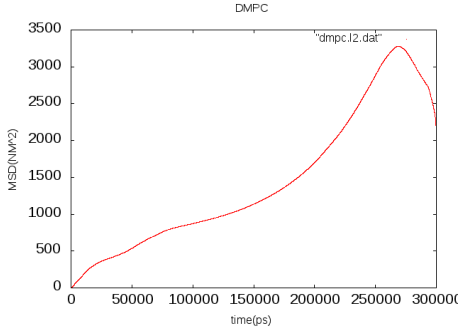

Figure 4.10: Mean square displacement V/s time for DMPC in the system Aβ(25-35) in bicelle

4.5.2 Molecular dynamics simulations of Aβ(1-40) in bicelle

Martini coarse grained force field was used for the molecular dynamics simulations. The simulation was run for $0.21\mu s$ at 298 K. Volume of the simulation box was $216\times10^3 nm^3$. 3 molecules of Aβ(1-40), 288 molecules of DMPC, 576 molecules of DHPC and 15000 water molecules constitute the system.

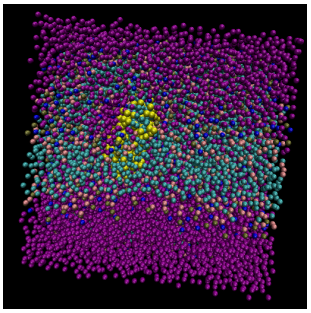

Figure 4.11: The system Aβ(1-40) in bicelle after simulation,pink:water, Aquamarine:Phospholipids, Yellow: Aβ(1-40)

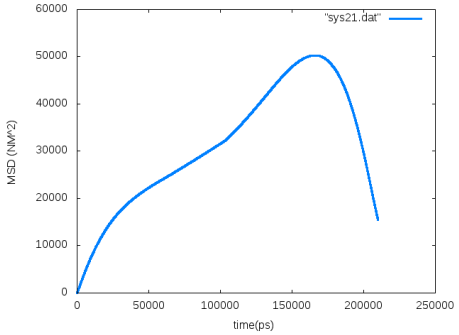

Figure 4.12: Mean square displacement V/s time for the system Aβ(1-40) in bicelle

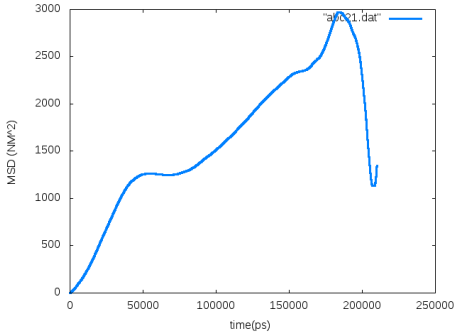

Figure 4.13: Mean square displacement V/s time for Aβ(1-40) in the system Aβ(1-40) in bicelle

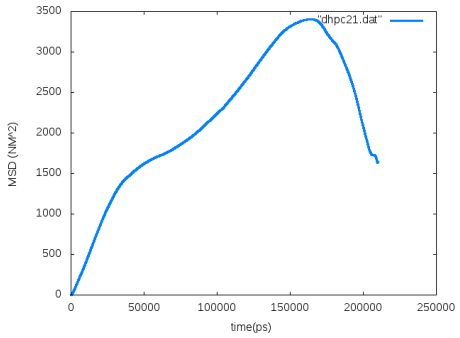

Figure 4.14: Mean square displacement V/s time for DHPC in the system Aβ(1-40) in bicelle

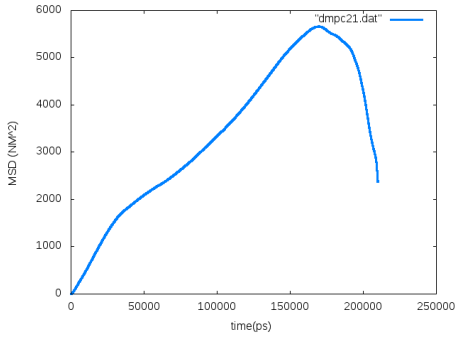

Figure 4.15: Mean square displacement V/s time for DMPC in the system Aβ(1-40) in bicelle

4.6 Conclusion

Molecular dynamics simulations can provide information about the macroscopic properties of a system. From the visualization of the final system it is clear that Amyloid beta will bind to the surface of the bicelle. The mean square displacement for both Aβ(25-35) in bicelle and Aβ(1-40) in bicelle show a non linear relationship with time. When Amyloid beta peptide is incorporated in bicelle it diffuses anomalously.

Chapter 5

Crowding Environment Experiments

5.1 Macromolecular Crowding

The term macromolecular crowding in biological systems is that the concentration of macromolecules is so high it will occupy a considerable volume and reduces the availability for other molecules. These effects can be originating from steric repulsion.[Ell01] Macromolecular crowding can alters the properties of proteins in the solution when the concentration of the molecules is very high. The intracellular volume is unavailable to other macromolecules depends upon the numbers, sizes and shapes of all the molecules present in each compartment.[Ell]
Protein aggregation is a high-order process whose rate is very sensitive to concentration.Crowding should favour aggregation because of its effect of increasing the thermodynamic activity of partly folded polypeptide chains.

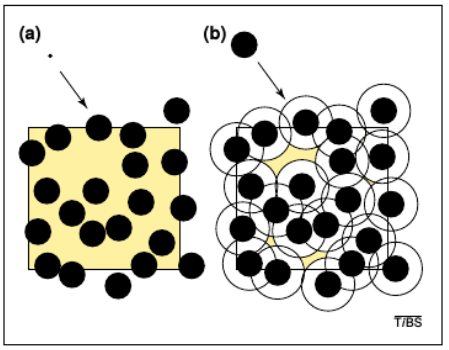

Figure 5.1: Reduced volume effect in macromolecular crowding. (taken from [Ell])

5.2 NMR Experiments

1D and 2D NMR experiments were conducted to study the change in the conformation of Aβ(25-35) in the presence of bicelle.
Sample: 2mM Aβ(25-35) in bicelle(DMPC/DHPC) with 2% crowding agent (PEG).

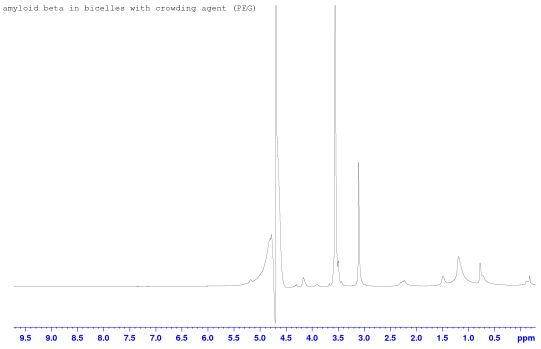

Figure 5.2: 1D NMR spectrum of Aβ(25-35) in bicelle in presence of crowding agents

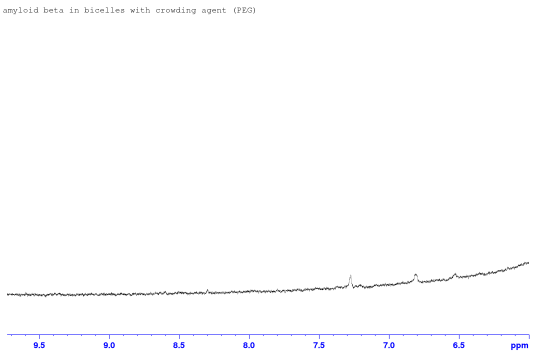

Figure 5.3: 1D NMR spectrum of Aβ(25-35) in bicelle in presence of crowding agents

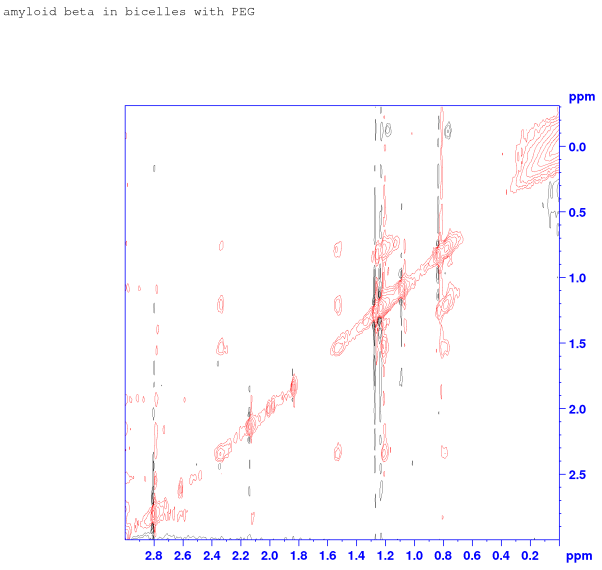

Figure 5.4: TOCSY of Aβ(25-35) in bicelle in presence of crowding agents

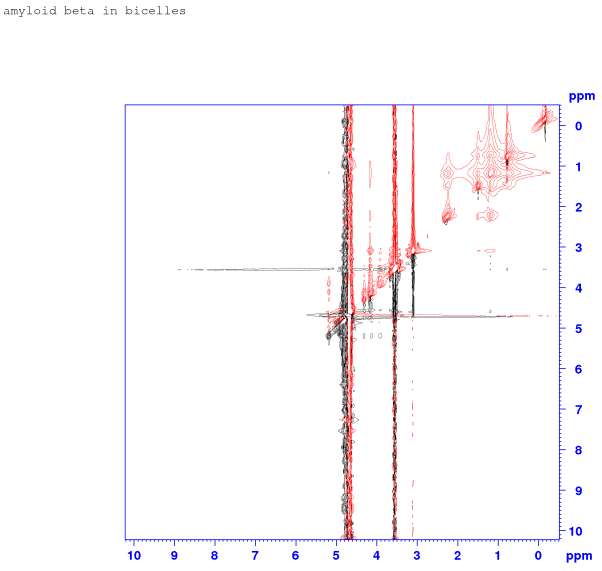

Figure 5.5: ROESY of Aβ(25-35) in bicelle in presence of crowding agents

Chapter 6

Summary and future directions

Our aim was to study the dynamics of diffusion of Amyloid beta peptide(25-35) inside a bicelle. As the first step we tried to confirm the structure of the Aβ(25-35) in the bicelle using 2 dimensional NMR experiments. Assignments of Aβ(25-35) in bicelle using the software SPARKY by inputting the chemical shifts inferred from the 2D NMR experiments.

The diffusion coefficient of Aβ(25-35) in bicelle, bicelle alone were calculated by pulsed field gradient (pfg) NMR and pfg NMR with water suppression. We observed a linear diffusion in Aβ(25-35) alone sample and bicelle alone sample. But when Aβ(25-35) was inserted into the bicelle it started following anomalous diffusion behaviour.

Molecular Dynamics simulations were performed for Aβ(25-35) in bicelle and Aβ(1-40) in bicelle using GROMACS. From the mean square displacement-time plots it was inferred that these systems show anomalous diffusion.

In future we will fit these experimental results to a defined anomalous diffusion model by quantifing the spatial heterogenity index α. α can provide information on the non linearity of mean square displacement and time.

In addition we want to study the folding mechanism and structure formation of Aβ(25-35) in a crowding environment created by macro molecular crowding agents Ficoll and PEG using NMR experiments and molecular dynamics simulations.

Appendix A

Commands used for GROMACS simulations

- Pdb2gmx : to convert pdb file into .gro file.
  - **Options**
    - -f : for an input file
    - -o : for an output file.
- genbox : generates a box of solvent.
  - **Options**
    - -cs : specified coordinates for the solvent.
    - -cp : specified coordinates for solute.
    - -ci : add molecules at random position.
    - -nmol : insert extra molecules.
    - -box : creates box with specified dimensions.
    - -try n : try 'n' times.
    - -maxsol : maximum nunber of solvent molecules.
- grompp : reads md files with input parameters.
  - **Options**
    - -c : checks whether the coordinate file is matching the topology file.

- Mdrun : performs molecular dynamics simulations.
  - **Options**
    - -v : uses verlet velocity integrator.
- g_msd : calculates mean square displacement.
  - **Options**
    - -lateral : calculates lateral diffusion coefficient.
- editconf : converts and manipulates structure files , edits the box.

Appendix B

Three letter codes for amino acids

Amino acides	Three letter code
Alanine	Ala
Arginine	Arg
Asparagine	Asn
Aspartic acid	Asp
Cysteine	Cys
Glutamine	Gln
Glutamic acid	Glu
Glycine	Gly
Histidine	His
Isoleucine	Ile
Leucine	Leu
Lysine	Lys
Methionine	Met
Phenylalanine	Phe
Proline	Pro
Serine	Ser
Threonine	Thr
Tryptophan	Trp
Tyrosine	Tyr
Valine	Val

Appendix C

Derivation of Stokes Einstein equation

Newtons equation of motion for a particle moving under a constant external force F in x direction,

$$\frac{dv_x}{dt} = \frac{F}{m} \tag{C.1}$$

v_x: velocity of the particle

m: mass of the particle

$$v_x(t) = v_{0,x} + \frac{Ft}{m} \tag{C.2}$$

$$\Delta x = v_{0,x} + \frac{F(\Delta t)^2}{2m} \tag{C.3}$$

Taking average for equation C.3 gives

$$< \Delta x >= \frac{F(\Delta t)^2}{2m} \tag{C.4}$$

[$< v_{0,x} >$ is zero since in each step it is pointing randomly towards left or right.] Because of friction the particle will attain a terminal velocity,

$$v_t = \frac{F}{f} \tag{C.5}$$

Where the viscous friction coefficient

$$f = \frac{2m}{\Delta t} \tag{C.6}$$

'f' for a spherical object is given by the Stokes formula.

$$f = 6\pi\eta R \tag{C.7}$$

η: viscosity [unit : Pa.s] R : hydrodynamic radius
From the 1D diffusion law diffusion coefficient D can be written as,

$$D = \frac{L^2}{2\Delta t} \tag{C.8}$$

Using equation C.7 and C.8 we could write

$$fD = \frac{mL^2}{\Delta t^2} \tag{C.9}$$

$$fD = mv_{0,x}^2 \tag{C.10}$$

From the equipartition of energy we can deduce that

$$< v_{0,x}^2 >= \frac{kT}{m} \tag{C.11}$$

$$\implies fD = kT \tag{C.12}$$

$$ie. D = \frac{kT}{f} \tag{C.13}$$

C.13 is known as Stokes Einstein relation.

Bibliography

[9] *Manual gromacs 4.5.6.*

[ABD10] Silvia Dante Alexandra Buchsteiner, Thomas Hauβ and Norbert A. Dencher, *Alzheimers disease amyloid-β peptide analouge alters the ps-dynamics of phospholipid membranes*, Biochimica et Biophysica Acta **1978** (2010), 1969–1976.

[Ber08] van Gunsteren W.F Berendsen, H.J.C., *Practical algorithms for dynamics simulations*, 2008.

[BM94] Banwell and McCash, *Fundamentals of molecular spectroscopy*, Tata McGraw Hill, 1994.

[Ell] R. John Ellis, *Macromolecular crowding: obvious but underappreciated*, TRENDS in Biochemical Sciences **26**.

[Ell01] R John Ellis, *Macromolecular crowding: an important but neglected aspect of the intracellular environment*, Current Opinion in Structural Biology **11** (2001), 114–119.

[Eva95] Jeremy N. S. Evans, *Biomolecular nmr spectroscopy*, Oxford University Press, 1995.

[Hoc74] Goel S.P. Eastwood Hockney, R. W., *Quiet high resolution computer models of a plasma.*, J. Comp. Phys. **14** (1974), 148–158.

[JC95] Arthur G. Palmer III Nicholas J. Skelton John Cavanagh, Wayne J. Fairbrother, *Protein nmr spectroscopy: Principles and practice*, Academic Press Inc, 1995.

[Kee02] James Keeler, *Understanding nmr spectroscopy*, Wiley, 2002.

[KMBH03] Raoqiong Bennet (Tong) Daniel B. Rowe Hanbing Lu Kevin M. Bennet, Kathleen M. Schmainda and James S. Hyde, *Characterization of continuously distributed cortical water diffusion rates with a stretched-exponential model*, Magnetic Resonance in Medicine **50** (2003), 727–734.

[KSU12] Oleg N. Antzutkin Vladimir V. Klochkov Konstantin S. Usachev, Andrey V. Filippov, *Spatial structure of beta-amyloid aβ 1-40 in complex with a biological membrane model, advances in alzeimers disease*, Advances in Alzeimers disease **1** (2012), 22–29.

[Lev07] Malcom H. Levitt, *Spin dynamics*, Wiley, 2007.

[MEC05] Massimo Coletta Federica Orsini Bruno Giardina Francesco Misiti M. Elisabetta Clementi, Stefano Marini, *Aβ(31-35) and aβ(25-35) fragments of amyloid beta-protein induce cellular death through apoptotic signals: Role of the redox state of methionine-35*, FEBS Letters **579** (2005), 2913–2918.

[Nel08] Philip Nelson, *Biological physics*, W. H. Freeman and Company, 2008.

[RG] Danielle Chandler Ramya Gamini, *Residue-based coarse graining using martini force field in namd*.

[RL11] Thomas Neuberger Andrew G.webb Richard L.Magin, Belinda S. Akpa, *Fractional order analysis of sephadex gel structures: Nmr measurements reflecting anomalous diffusion*, Non linear Science and Numerical Simulations **16** (2011), 4581–4587.

[SB05] Paul Schanda and Bernhard Brutscher, *Very fast two-dimensional nmr spectroscopy for real-time investigation of dynamic events in proteins on the time scale of seconds*, JACS **127** (2005), 8015–8016.

[Ser00] Louise C. Serpell, *Alzheimer's amyloid fibrils: structure and assembly*, Biochimica et Biophysica Acta **1502** (2000), 16–30.

[Sin12] Davy Sinnaeve, *The stejskal-tanner equation generalized for any gradient shape-an overview of most pulse sequences measuring free diffusion*, Concepts in Magnetic Resonance Part A **40A** (2012), 49–65.

[SV01] M. Aksenova C. Lauderback D.A. Butterfield S. Varadarajan, J. Kanski, *Different mechanisms of oxidative stress and neurotoxicity for alzheimer's aβ(142) and aβ(2535)*, J. Am. Chem. Soc. **123** (2001), 5625–5631.

[TLLS06] Deborrah J. Tew Roberto Cappai Colin L. Masters Gerardo D. Fidelio Kevin J. Barnham Tong-Lay Lau, Ernesto E. Ambroggio and Frances Separovic, *Amyloid-β peptide, disruption of lipid membrane and effect of metal ions*, Journal of molecular biology **359** (2006), 759–770.

[uR08] Atta ur Rahman, *Nuclear magnetic resonance*, Springer, 2008.

[V.B08] V.Balakrishnan, *Elements of non equilibrium statistical mechanics*, 2008.

[YYG10] Young-Ho Lee Takahisa Ikegami Eri Chatani Hironobu Naiki Yuichi Yoshimura, Kazumasa Sakurai and Yuji Goto, *Direct observation of minimum-sized amyloid fibrils using nmr spectroscopy*, Protein Science **19** (2010), 2347–2355.

[Zwa01] Robert Zwanzig, *Nonequilibrium statistical mechanics*, Oxford university press, 2001.